Constraints on Enhanced Weathering and related carbon sequestration – a cropland mesocosm approach

[1]Thorben Amann, [1]Jens Hartmann, [2]Eric Struyf, [1]Wagner de Oliveira Garcia, [3]Elke K. Fischer, [4]Ivan Janssens, [2]Patrick Meire, [2]Jonas Schoelynck

5 [1]Institute for Geology, Center for Earth System Research and Sustainability, University of Hamburg, Germany
[2]University of Antwerp, Department of Biology, Ecosystem Management Research Group, Universiteitsplein 1C, B-2610 Wilrijk, Belgium
[3]Institute of Geography, Center for Earth System Research and Sustainability, University of Hamburg, Germany
[4]University of Antwerp, Research Centre of Excellence Global Change Ecology, Universiteitsplein 1, B-2610 Wilrijk, Belgium

10 *Correspondence to*: Thorben Amann (science@thorbenamann.de)

Abstract. The weathering of silicates is a major control on atmospheric CO_2 at geologic time scales. It was proposed to enhance this process to actively remove CO_2 from the atmosphere. While there are some studies that propose and theoretically analyze the application of rock powder on agricultural land, results from field experiments are still scarce.

In order to evaluate the efficiency and side effects of Enhanced Weathering, a mesocosm experiment was set up and agricultural

15 soil from Belgium was amended with olivine-bearing dunite ground to two different grain sizes, while distinguishing setups with and without crops.

Based on measurements of Mg, Si, pH, and DIC, the additional weathering effect of olivine could be confirmed. Calculated weathering rates are up to three orders of magnitude lower than found in other studies. The calculated CO_2 consumption by weathering was comparably low with 2.3 - 4.9 CO_2 t km^{-2} a^{-1}. One identified cause was preferential flow leading to a low

20 water-rock interaction time for a significant water volume in the setup, not addressed in previous Enhanced Weathering experiments for CO_2 consumption. Correction for preferential flow leads to fluxes about a magnitude higher, confirming that this process and surface runoff in the field must be included in assessments for the CO_2 consumption potential of Enhanced Weathering in general. Pore water Mg/Si molar ratios suggest that dissolved Si from the added minerals stays in the system over the observation period, because a cation depleted Si layer forms on the reactive mineral surface of freshly ground rocks.

25 This layer has not reached equilibrium thickness within the first two years.

The release of potentially harmful trace elements is an acknowledged side effect of Enhanced Weathering. Primarily Ni and Cr are elevated in soil solution, while Ni concentrations exceed the limits of drinking water quality. The use of olivine, rich in Ni and Cr, is not recommend and alternative rock sources are suggested for the application.

1 Introduction

The application of rock powder on agricultural soils has long been used to improve soil properties to achieve a productivity increase (De Villiers, 1961; Kronberg, 1977; Leonardos et al., 1987; Anda et al., 2015a, 2013; Anda et al., 2015b; Shamshuddin and Anda, 2012) the practice effectively dates back thousands of years (Lightfoot, 1996) and is still used in modern agriculture,

5 predominantly in the form of liming. The application of carbonate rock powder to agricultural soils is a process to adjust soil pH (Cregan et al., 1989) and to increase crop production (Haynes and Naidu, 1998). Besides pH adjustment, the additional release of cations and anions into the soil-rock system alters the chemical composition of the soil solution. However, alternative amendment materials are gaining increased attention, one of which is the addition of silicate rock powder. Silicate rocks can be applied to provide geogenic nutrients via the chemical weathering of the additional minerals (Hartmann et al., 2013; Van

10 Straaten, 2006). On top of that, it has the strong additional advantage of providing the potential for enhanced atmospheric CO_2 sequestration: on geological time scales, natural silicate weathering is one of the most important controls on atmospheric C concentrations over geologic time scales (Berner, 2003). Enhanced silicate weathering (EW) has therefore been put forward as a technique with strong potential to contribute to climate mitigation: in order to achieve COP21 atmospheric CO_2 concentration targets, it becomes more likely that not only emission reduction is required (Fuss et al., 2014; Rogelj et al., 2018;

15 Peters, 2016). Focus should also be put on applying effective CO_2 sequestration techniques (Sanderson et al., 2016; Beerling et al., 2018; Minx et al., 2018).

With dwindling resources of rocks with concentrated content of widely applied macro-nutrients, which might lead to a shortage of traditional fertilizers (Cordell et al., 2009; Manning, 2015), geogenic nutrient replacement by enhanced weathering will become a valid alternative to supply not only phosphorus or potassium but also further geogenic nutrients, with potentially

20 important local impact on food security (van Straaten, 2002; Cordell et al., 2009). In addition, alternative regional fertilizer concepts for certain regions need to be developed to enhance productivity, as for example in Africa (Ciceri and Allanore, 2019).

However, the application of silicate rock products requires knowledge of soil mineral properties, hydrology, soil solution composition, and element uptake by plants to enable predictions on its consequences. Specifically this knowledge is lacking

25 at the broader scheme (Beerling et al., 2018; Beerling, 2017; Kantola et al., 2017; Edwards et al., 2017; Taylor et al., 2017), despite several experiments in the past (Anda et al., 2015a, 2013; Shamshuddin and Anda, 2012; Shamshuddin et al., 2011). One of the main gaps is the evolution of soil solution composition and its migration in the treated soil, considering a broad variety of possible combinations of soil type, rock product, and plant species (Hartmann et al., 2013). The time scale at which changes in weathering fluxes can be expected at the scale of large catchments was shown for the Mississippi, where alkalinity

30 fluxes increased by more than 50% over less than a century, which was partly attributed to liming and land management processes (Raymond and Cole, 2003; Raymond and Hamilton, 2018). In general, past land use change and management of catchments can affect the chemical baselines of rivers draining to the ocean over decades (Hartmann et al., 2011; Hartmann et

al., 2007; Meybeck, 2003; Radach and Pätsch, 2007). The large-scale application of rock products will likely lead to an alteration of river chemistry, and consequences for adjacent coastal zones remain to be assessed.

In the future, increasing food and bioenergy demand will probably lead to more efforts to improve soil conditions for optimized biomass production (Fuss et al., 2018). The future application of customized rock products to provide slow release geogenic

5   nutrient fertilizers, adjust pH, increase cation exchange capacities (CEC), or adjust soil hydrology is therefore likely. The replenishment of geogenic macro- and micronutrients is needed because the natural supply cannot keep up with the permanent removal from the soil-rock system under intensive harvest scenarios for crops or timberland (de Oliveira Garcia et al., 2018; Van Straaten, 2006). The application of rock products will therefore change the fluxes of elements within the soils, while being mediated by the biological pump.

10 One of the key issues is the dissolution rate of applied rock material. While the kinetics are relatively well understood at the laboratory scale for singular minerals (Rosso and Rimstidt, 2000; Wogelius and Walther, 1992), the dissolution rate of a rock powder mixture, with fresh surfaces, which had not been in contact with an aquatic phase before, is relatively unknown. Several points of the rock powder application on soils have to be considered. First, the upper parts of soils are not permanently saturated with water, which may lead to dissolution-precipitation reactions. Second, it can be expected that mineral surfaces initially

15 need to equilibrate with the new system and varying water content, and that dissolution rates of minerals will be different from those being in long-term equilibrium within the natural soil system. Third, trace elements from the applied rock material will eventually be released and migrate downwards, reprecipitated if oversaturation with a specific mineral phase occurs, and adsorbed to soil minerals or organic matter.

To understand these processes in an agricultural setting with typical crops, dunite could serve as model rock material,

20 containing often by more than 90% of olivine, a mineral often used as model mineral to theoretically study effects of Enhanced Weathering (Schuiling and Krijgsman, 2006; Hartmann et al., 2013; Köhler et al., 2010; Taylor et al., 2015; Renforth et al., 2015; Montserrat et al., 2017). In our present study, we applied dunite to agricultural soils to quantify the impact on inorganic carbon and dissolved silica fluxes in the presence and absence of crop plants. Dunite contains predominantly olivine, a low complexity mineral (inosilicate), compared to e.g. basalt, which has a much greater complexity (considerable quantities of

25 plagioclase and pyroxene, and to a lesser extent olivine and other trace minerals). In addition, basalt has the potential to provide the nutrient phosphorus, which is typically not represented in large quantities in dunite. The release of phosphorus could potentially influence plant-weathering interactions in the soil, complicating the analysis of the weathering process.

We studied the release of the major elements Mg and Si predominantly derived from Mg-olivine, and assessed whether dissolution occurs stoichiometrically, or whether a secondary layer covering the fresh surfaces of minerals will develop,

30 potentially enriched in Si and depleted in Mg (Daval et al., 2013a; Hellmann et al., 2012; Pokrovsky and Schott, 2000). In addition, the release of trace metals was used to understand dissolution processes. Nickel (Ni) in olivine is expected to be released as it substitutes for Mg. Chromium (Cr) on the other side, as chromite, or sometimes chromochlorite, present in dunite, is not expected to be released strongly at the observed pH levels in the system.

2 Methods

2.1 Mesocosm setup

In October 2013, a fully-replicated setup (five replicates per treatment combination) of mesocosms was built up and left running for 730 days. Here we report on data of the first year. Rain barrel type mesocosms with a diameter of 46 cm were

5 filled with a natural loamy soil from Belgium (detailed characterisation in supplement S1). Controlled factors were the application of olivine in the top layer of the soils (22 kg m^{-2}) using two different olivine grain size fractions (coarse sand and fine sand to silt), two crop plants (wheat and barley) and two rain regimes (daily and weekly precipitation), while the total amount of rain was the same (adjusted to about 800 mm a^{-1}). Controls were established by using the same setup without olivine application (blanks) and without plants. Soil solutions were sampled at roughly 10, 20, and 30 cm depth and at the bottom of

10 the mesocosms (Fig. 1).
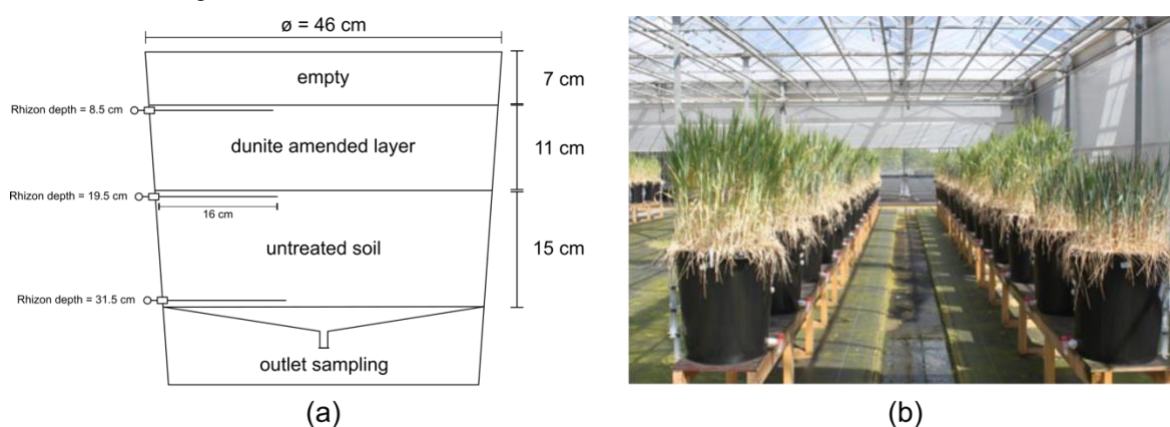
Fig. 1: (a) Schematic mesocosm configuration; (b) status of the experiment in April 2014.

2.2 Material

The experiment material was produced from dunite rock, containing approximately 85% olivine, of which 92% are forsterite (Mg endmember olivine). The rest is comprised of lizardite (Mg-rich serpentine, Cr containing chlorite (including chromite or chrome-spinell inclusions) and traces of chabazite (zeolite group) and Mg-hornblende (amphibole), determined by energy

15 dispersive x-ray spectrometry (Zeiss LEO 1455 VP coupled with an EDX detector by Oxford Instruments). It originates from an Åheim mineral deposit (North Cape Minerals Company, Norway). The bulk chemical composition (Panalytical Magix Pro wavelength dispersive X-ray fluorescence (XRF) analysis) of the sample is given in Tab. 1. The material was supplied in two grain size classes, a fine and a coarse fraction (Tab. 2). The sample was analyzed for specific surface area, measured using N$_2$ and Kr adsorption during BET analyses (Brunauer et al., 1938) with a Quantachrome autosorb iQ (Tab. 2), and for the particle

20 size distribution (using Sympatec Helos KFMagic laser granulometry). The specific surface area of the fine grain size product is almost one order of magnitude larger than the coarse grain size product.

Tab. 1: Geochemical composition of source dunite, derived from XRF runs (n=3).

Oxide	mass-%	s.d.	Element	mass [mg kg^{-1}]	s.d.
SiO$_2$	40.14	0.05	Ba	55	9
Al$_2$O$_3$	0.70	0.01	Ce	8	1
Fe$_2$O$_3$	6.75	0.01	Co	105	2
MnO	0.09	0.00	Cr	2156	3
MgO	44.99	0.25	Cu	13	2
CaO	0.40	0.00	Ga	3	1
Na$_2$O	0.03	0.00	La	0	0
K$_2$O	0.06	0.00	Nb	1	1
TiO$_2$	0.01	0.00	Nd	29	5
P$_2$O$_5$	0.01	0.00	Ni	2889	18
SO$_3$	0.00	0.00	Pb	1	1
LOI	6.48	0.00	Rb	4	2
total	99.68		Sc	9	1
			Sr	56	1
			Th	1	2
			U	5	4
			V	31	3
			Y	3	1
			Zn	36	2
			Zr	0	0

Tab. 2: Specific surface area of the source material, derived by BET analyses, as well as grain size distribution characteristics. [a]sieve mesh at which 20% are retained, thus 80% being smaller than the given diameter; [b]class with the largest class weight; [c]this class is divided into five smaller classes but was summed to show the share below 1 µm.

grain size category	Specific surface area, N based [m^2 g^{-1}]	Specific surface area, Kr based [m^2 g^{-1}]	p80[a] [µm]	dominating class[b] [µm]	Share of dominating class [%]	Smallest class [µm]	Share of smallest class [%]
fine	9.53±0.43	14.75±0.24	43.5	25.5	6.7±0.02	< 0.9[c]	2.66±1.51
coarse	1.06±0.10	1.61±0.03	1020	720	10.8±0.7	< 18	1.51±0.03

2.3 Analysis

2.3.1 Silica and magnesium

The sampled water was filtered through 0.45 µm nitrocellulose Chromafil syringe filters (A-45/25) into sample bottles and stored cool (4°C) until chemical analysis for dissolved silica (Si) and Magnesium (Mg) on an inductively coupled plasma atomic emission spectrophotometer (ICP-AES, Thermo Scientific, ICAP 6000 Series).

2.3.2 pH

The pH in the outlet sampling water was measured using a WTW pH meter, calibrated with three points using NIST buffer standards (pH 4, 7, and 10).

2.3.3 Trace metals

In the soil solution as well as in the soil material, concentrations of aluminium (Al), barium (Ba) chromium (Cr), cobalt (Co), iron (Fe), manganese (Mn), nickel (Ni), strontium (Sr), and zinc (Zn) were analysed using inductively coupled plasma atomic emission spectroscopy (ICP-AES, Optima 2100, Perkin Elmer). For analysis of the total content of substances within the soil

5   material, a digestive procedure was done according to Heinrichs and Herrmann (2013). In brief, soil was dried at 40°C and milled with a planetary ball mill. 150 mg of soil was weighed into teflon crucibles and a mixture of 4 mL nitric acid (65 % *Suprapur* grade), 2 mL hydrofluoric acid (40 % *Suprapur* grade) and 2 mL perchloric acid (70 % *Suprapur* grade) was added. The crucibles were sealed and placed for 10 h in a closed digestion aperture (*PICOTRACE*) at 170°C to ensure complete dissolution. Subsequently, the acids were vaporised in a closed system and the residues were dissolved with 2 mL nitric acid

10   (65 % *Suprapur* grade), 0.6 mL hydrochloric acid (37 % *Suprapur* grade) and 20 mL high-purity water at 90°C for 1 h. The solutions were standardised to 50 mL with high-purity water and underwent Optical Emission Spectroscopy (ICP-OES) as described above.

2.3.4 Dissolved inorganic carbon (DIC)

DIC was measured with a Picarro G2131-i cavity ring-down spectrometer coupled to a preparation device (AutoMate FX, Inc.)

15   for discrete sample measurement.

3 Results

3.1 Hydrology

The experiment was set up to be treated with two rain regimes, continuous and intermittent treatment. Since there were no significant differences between results of both rain treatments, all discussed data contain values from both. After the experiment

20   start, it took between 7 and 23 days until water reached the bottom of the mesocosms. Water collected at the outlet of each pot can be used to estimate the loss of water trough evaporation and transpiration. Data clearly shows elevated evapotranspiration in the mesocosm seeded with crops (Fig. 2). Vice versa, less outflow volume is measured especially in times of strong plant growth. Sample volume which could be extracted varied. Between days 200 and 300, growth of plants and elevated ambient temperatures caused strong evapotranspiration, which reduce the outflowing water volume to a minimum. At these times, no

25   or only a little sample volume could be obtained.
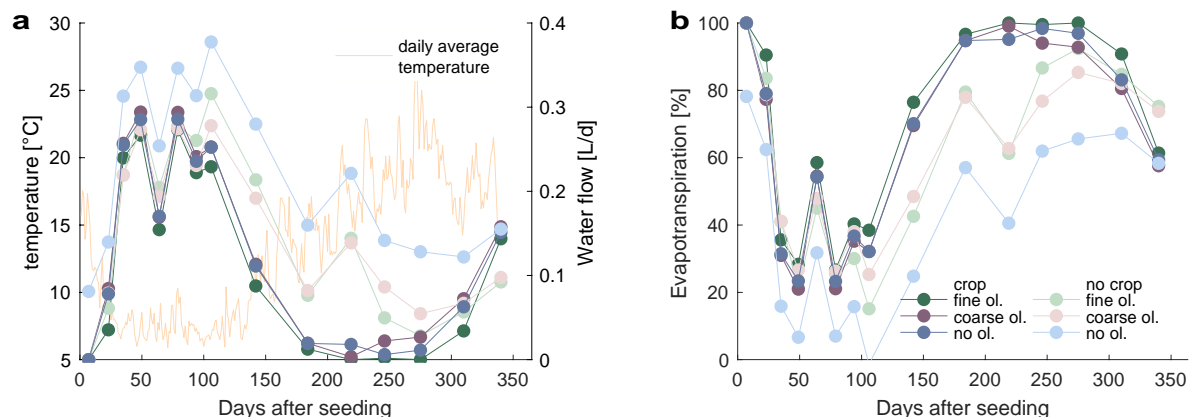
Fig. 2: a) Average daily temperature in the greenhouse and water flow from outlet, values refer to daily fluxes from the preceding interval. b) Relative evapotranspiration, calculated from the difference of precipitation input and pot outflow, relative to precipitation.

3.2 Release patterns of weathering tracers

Elevated concentrations of the major studied parameters DIC, Mg, and Si are only observed in the uppermost layers, with the largest increase in the top layer if compared to the base level setup without olivine. Changes in DIC and Mg concentrations are most pronounced in the mesocosms supplied with fine dunite material, with values markedly above base concentrations in

5   the setup with coarser dunite (Fig. 3, Fig. 5). A pronounced increase of pH in the beginning of the experiment (Fig. 4), with values near 9 for the fine grain size setup, can be observed. Observed pH values decrease over the course of the experiment to approximately 8. Depending on the setup, the pH in the fine setup is about 0.5 pH units higher than in the others after two years. Si concentrations develop dissimilarly, with most pronounced increases in the coarse setup whereas the fine setup releases less than half of the Si into the soil solution in the surface level (Fig. 6). The effect is less obvious in the second layer

10   and no changes are visible below. Interestingly the Si concentrations in the top layer for treatments with the fine material are also lower than if no olivine was supplied. With the exception of visible differences in Si concentrations, with lower values in the setups with plants, no clear difference pattern can be identified if crop plants are present (Fig. 3 - Fig. 6). For DIC in fine material treatments the concentrations tend to be higher in the first year in the top layer where data were available. Not at all sampling times, enough sample volume was available for DIC analyses, as priority was given to other major compounds. The

15   general pattern is a large variation in concentrations suggesting that the variability between mesocosms is high and that five replicas per setup are probably not enough to derive a differentiated signal as presented for the major element concentrations. Despite the large variability, it is clear that the weathering signal from the applied dunite travels slowly downwards. Within the first year, it was not moving much beyond the 20 cm level, as elevated Mg concentrations, which provide the clearest signal for olivine dissolution, were not clearly detectable at the third level (30 cm), with two exceptions in case of the fine

20   grain setup.
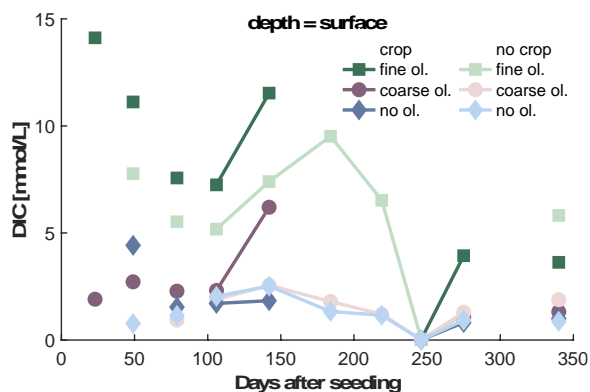
Fig. 3: Development of average DIC concentrations over one year in the surface layer, differentiated by olivine and crop treatment. For more information on the subsequent layers and error bars, please refer to supplement Fig. S3. Data gaps (line discontinuities) occur where samples were taken but no analysis was done.
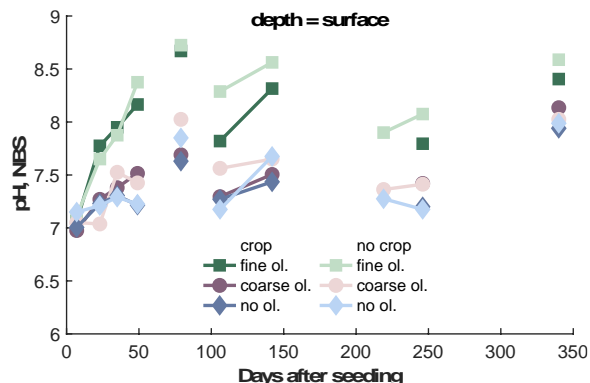
Fig. 4: Development of pH values (averaged proton concentrations, converted to pH) over the experiment period in the surface layer, differentiated by olivine and crop treatment. For more data and error bars, please refer to supplement Fig. S4. Data gaps (line discontinuities) occur where samples were taken but no analysis was done.
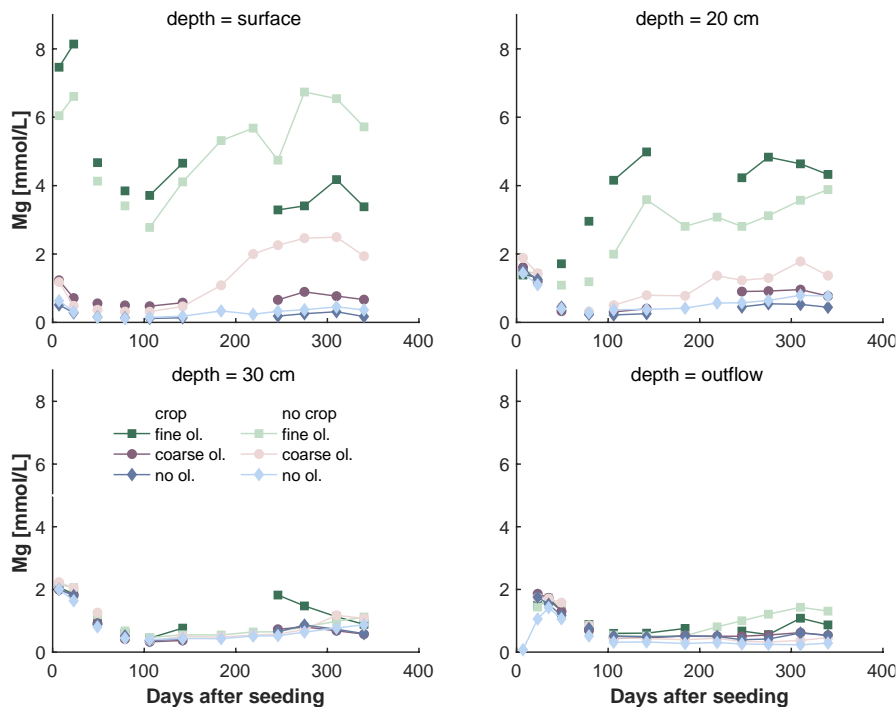
Fig. 5: Development of Mg concentrations over the experiment period, differentiated by olivine and crop treatment. For more differentiated data and error bars, please refer to supplement Fig. S5. Data gaps (line discontinuities) occur where samples were taken but no analysis was done.
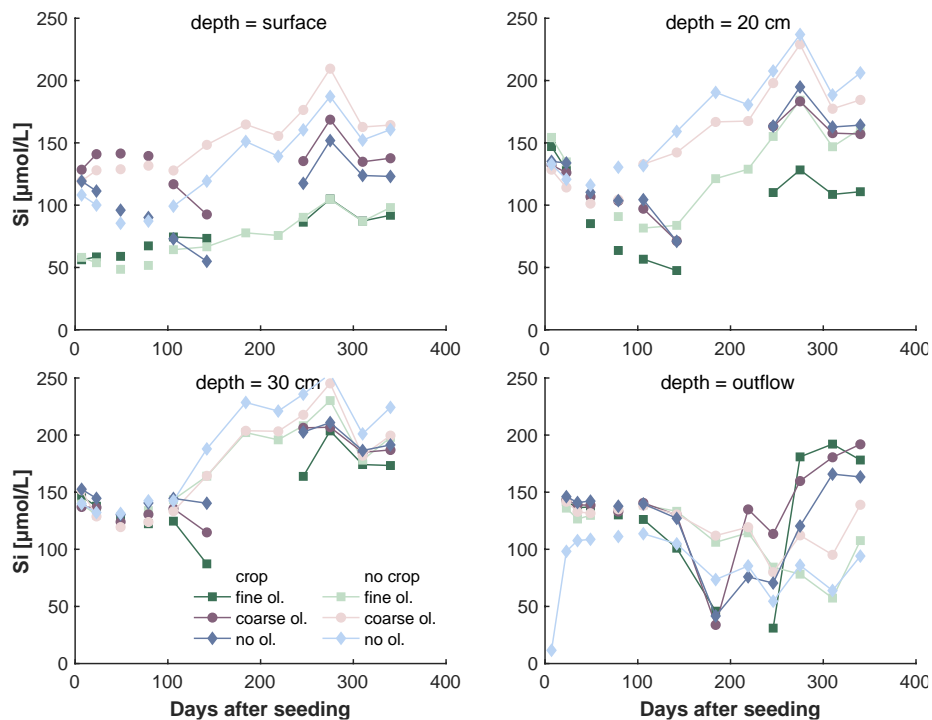
Fig. 6: Development of Si concentrations over the experiment period in the surface layer, differentiated by olivine and crop treatment. For more differentiated data and error bars, please refer to supplement Fig. S6. Data gaps (line discontinuities) occur where samples were taken but no analysis was done.
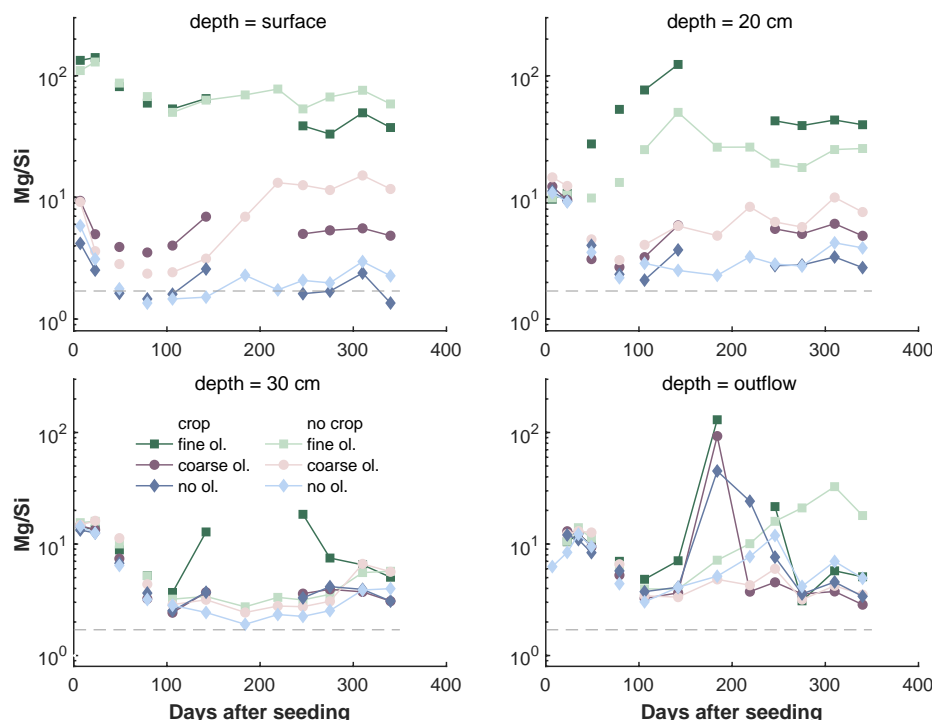
Fig. 7: Development of Mg/Si ratios over the experiment period in the surface layer, differentiated by olivine and crop treatment. The dashed grey line indicates the stoichiometric Mg/Si ratio of 1.7 based on the rock chemistry. For more differentiated data and error bars, please refer to supplement Fig. S7. Data gaps (line discontinuities) occur where samples were taken but no analysis was done.

Due to the low Si and high Mg concentrations, the Mg/Si ratio is elevated in the upper two levels of fine grain treatment, and less distinguishable for the coarse grain treatments. Shortly after the start of the experiment Mg/Si ratios (Fig. 7) in the first layer of the fine grain treatment are high (Mg/Si > 50), due to strong increase of Mg and the comparably low increase of Si. The effect is weaker for the coarse grain treatment (Mg/Si < 30, but still above 2). There is no distinct difference in the three

5 setups (fine, coarse, no dunite) in the deepest layer and the outlet. Generally, Mg/Si is clearly above 2 for the upper two layers, which are amended with olivine. The ratio is in the range of 1-10 in the unaffected layers and in the setup without olivine (Fig. 7). There is an increase in Mg and Si concentrations and other elements until about day 250, from drying-up during the warm period in the greenhouse caused by evaporation and evapotranspiration under presence of plants, resulting in low soil water content.

10 **3.3 CO_2 sequestration rates**

The additional CO_2 consumption by olivine amendment can be based on the release of Mg^{2+}, considering the average geochemical composition of the material and the background values from applied soils and irrigation water. Based on the stoichiometric composition, the ideal dissolution of 1 mol Mg-olivine yields 2 mol Mg and consumes 4 mol CO_2. The ability

to sequester atmospheric CO_2 is material specific and depends here on the Mg^{2+} that can be released during hydrolysis from the Mg-rich olivine. It is defined as the carbon dioxide removal RCO_2 in tons of CO_2 per ton of forsterite (estimated to be 1.1 for ultramafic (i.e. Mg rich) rocks (Moosdorf et al., 2014)). This assumption is considering that impurities and equilibration effects reduce the theoretical maximum RCO_2 of 1.25 for forsterite. CO_2 sequestration rates can then be calculated by

$$CO_2 \; sequestration = \frac{\sum Flux_{Mg^{2+}} \times molweight_{Mg}}{fraction \; of \; Mg \; in \; Forsterite} \times RCO_2 \qquad (1)$$

5   Details on the calculation Mg fluxes can be found in supplement section S14.

Calculating the average of Mg concentrations over the first year (340 days) of the experiment without consideration of the preferential flow effect, results in a total annual CO_2 sequestration of 2.3 - 4.9 t CO_2 km^{-2} a^{-1} depending on the applied grain size (Tab. 3).

To estimate the order of magnitude of the preferential flow effect, Mg concentrations in the outlet water can be compared to

10   those in the surface layer pore water, assuming that all Mg in the outlet sample is coming from the olivine in the surface layer. Coarse setups show a ratio of 12.2 and fine a ratio of 13.8 (Tab. 3),

Tab. 3: Mg and water flux averages (± SD) throughout the period of the experiment, excluding background contributions from soil and irrigation water. Includes crop and no crop treatment data. Detail on the calculation of CO_2 consumptions are found in supplementary section S14.

	Mg [μmol L^{-1}]		ratio[a], to account for preferential flow	Water flux at outlet [L d^{-1}]	CO_2 consumption [t km^{-2} a^{-1}]	
	surface layer	outlet material			based on flux at outlet	factoring in preferential flow[b]
fine	4713.1 ± 1128.2	357.8 ± 238.1	13.8 ± 7.4	0.8 ± 0.6	4.9	67.6
coarse	792.7 ± 516.2	139.6 ± 117.1	12.2 ± 6.6	0.9 ± 0.6	2.3	28.0

[a]Calculated directly from original Mg concentrations (not averages). Data were taken only from day 79 onwards because fluctuations were too inconsistent in the first weeks of the experiment. [a]CO_2 consumption from outlet multiplied with ratio to account for preferential flow.

15   **3.4 Trace metals**

3.4.1 Soil

Analyses of the soil elemental composition shows that some trace element concentrations are elevated, where olivine was applied (Fig. 8). Markedly, this is the case for Co, Cr, Ni, Mn, Al and Fe. There are no expressed differences between the applied grain sizes and crop types.
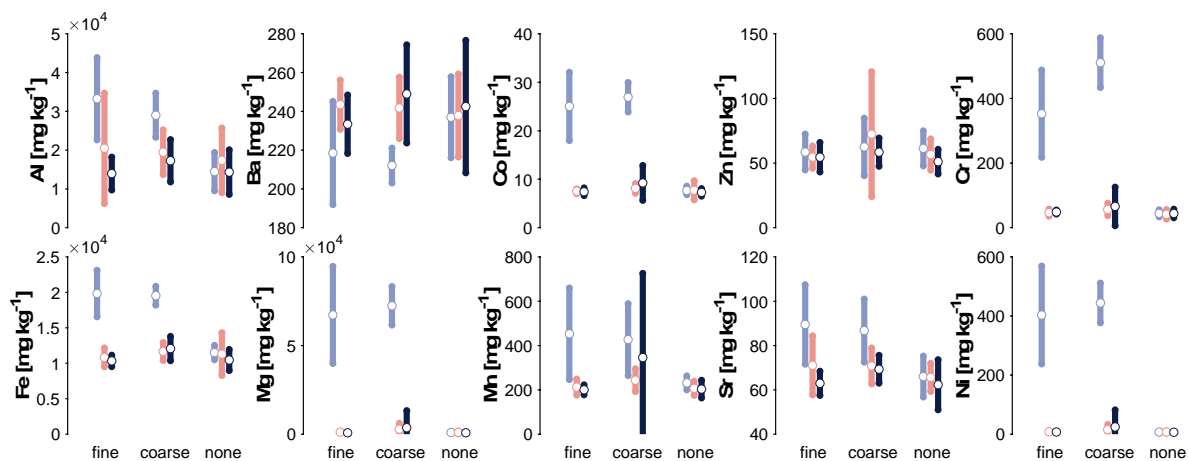
Fig. 8: Averaged trace element concentrations in the soil material, differentiated by olivine treatment (grouping) and depth (blue: surface, red: middle, black: bottom). Error bars indicate 1SD. Find data separated by plant type in supplement section S9.

3.4.2 Soil solution

Ni and Cr concentrations in the soil solution are elevated in the surface layer where fine olivine grain sizes were applied (Fig. 9) during the first 100 days. The coarse grain setup does not show any visible Cr concentration difference compared to the control, Ni concentrations in pots amended with olivine are higher than in the mesocosms without olivine on average (Fig. 9).

5 For the shallow concentrations, the existence of plants does not cause a distinct pattern for each setup compared to no plant treatments (supplement Fig. S9). Base values of Cr without olivine treatment are already above 50 nmol L^{-1}.
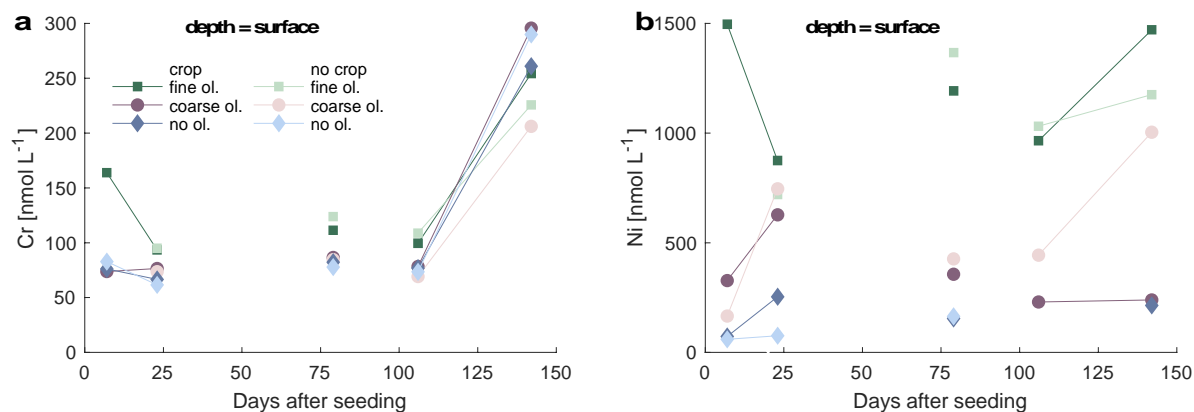
Fig. 9: Development of Cr (a) and Ni (b) concentrations over one year in the surface layer, differentiated by olivine and crop treatment. For more data and error bars, please refer to supplement Figs. S8 and S9.

For the other trace elements, no distinct pattern between treatments with and without olivine were identified apart from a general variability found in the solutions.

4 Discussion

4.1 Tracing the weathering effect

The fine olivine fraction shows about a ninefold higher specific surface area in both krypton- and nitrogen-based measurements than the coarse fraction (Tab. 2). This difference has implications for the release rate of elements as it is proportional to the available surface area under water saturated conditions. Averages of the first period show for Mg, with the clearest dissolution signal, a strong difference between Mg/Si release ratios of fine and coarse material setups, suggesting that the dissolution of the dunite and predominantly olivine is clearly not ideal if compared to standard laboratory kinetic experiments. Due to the precipitation of a secondary cation depleted amorphous silica layer around the fresh grains no initial strong release effect from fresh surface area is observed for silica. On the contrary, in the upper layer, concentrations of Si are lower in mesocosms treated with finer material than in those with coarser material (and even without olivine treatment, Fig. 6). Further effects are related to the distribution of water in the pore space, which is steered by grain size distribution effects, via differences of the water contact time with grain surfaces.

Based on the released Mg and BET surface area measurements of the dunite material, weathering rates can be estimated (details in supplement section S14). Derived rates are about a magnitude lower than values calculated for a soil column experiment and about three orders of magnitude lower than theoretical optimum dissolution rates (Tab. 4). These differences are not unexpected, considering that our experimental setup simulates natural processes like extended periods of drying out and subsequent slowed down or ceased chemical weathering processes.

Tab. 4: Calculated weathering rates of olivine, based on Mg release, compared to literature values.

	R (mol Ol m^{-2} s^{-1})	remark
This study[a]	$10^{-13.1}$ / $10^{-13.7}$	coarse/fine treatment, annual average
Renforth et al. (2015) [b]	$10^{-12.7} - 10^{-11.8}$	over the course of the experiment
Strefler et al. (2018) [c]	$10^{-10.7} - 10^{-9.8}$	at pH 7-9, min and max

If the Mg/Si ratio is two, the ideal stoichiometric molar ratio of element release from forsteritic olivine is reached. In the case of the applied material, the ratio is about 1.7 (based on RFA results). The experimental data show that Si and Mg in the upper layer are often decreased if plants are present (Fig. 5, Fig. 6). But even with this effect, Mg/Si ratios are still far from the equilibrium of 1.7. This effect is widely recognised as incongruent dissolution (Casey et al., 1993; Ruiz-Agudo et al., 2012). Considering that there are large amounts of Mg released, Si determines the ratio as no significant additions in the plants were observed. This shows that there is an active retention of Si, potentially leading to a cation depleted amorphous silica layer growing around the olivine minerals (Daval et al., 2013b; Daval et al., 2011; Hellmann et al., 2012). This effect has been described in detail for forsterite by Maher et al. (2016). High Mg/Si ratios indicate that in the beginning of the experiment the dissolution rate is controlled by the exchange of protons for Mg, while declining ratios over the course of the experiment indicate an approach to steady-state conditions (Maher et al., 2016). Since this effect eventually determines the CO_2

sequestration capacity, an estimation of the extent of those layers would lead to a better understanding of weathering kinetics. From the mesocosm experiments, it is only feasible to calculate a rough first order estimate given the rather crude setup of the mesocosms and should be improved in a future step. Calculated amorphous layer growth rates (details in supplement section S15) for the mesocosms without plants range from 0.02 nm a^{-1} (fine setup) to 0.08 nm a^{-1} (coarse setup). These values are

5   above or near the range of observations of surface layers in "aged" minerals, e.g. from Hellmann et al. (2012): 14.7 ka old feldspar with a surface layer of 50 nm ($\approx$ 0.0034 nm a^{-1}) and a layer of 150-200 nm on a younger (assuming 10 ka) serpentine ($\approx$ 0.02 nm a^{-1}). However, if assuming that the fresh surfaces of the forsterite are weathering faster in the beginning and a decrease in reaction rate can be caused by the formation of the amorphous layer due to processes related to the diffusion of released elements through the layer (Nugent et al., 1998; Daval et al., 2013b), this might explain why the calculated growth

10   rates are comparable to aged material. However, the experimental setup does not allow a more precise determination of these processes.

The formation of a depletion layer through the reprecipitation of Si alone cannot explain why Si concentrations in the fine setup are two to threefold below values of the control setup without olivine. We hypothesise that the increased release of Si from the finest grains leads to short term oversaturation of Si (about 1.9 mmol L^{-1} at 25°C; Stumm and Morgan (1996)), which

15   is followed by the formation of clay minerals such as smectites (Prudêncio et al., 2002) or by a mixture of different hydrous silicates of iron and magnesium, known as iddingsite (Smith, 1987).

4.2 CO$_2$ sequestration by olivine amendment

The pH of soil solutions increases by up to 1.0 and 0.3 pH units in mesocosm treated with fine and coarse olivine respectively (supplement Fig. S14). The effect is most pronounced in the upper layer and the first six months of the experiment, indicating

20   an enhanced reaction with the added rock powder, which contains a large fraction of very fine material, providing an increased reactive surface area. The effect indicates the generation of alkalinity by chemical weathering consuming CO$_2$ and can partly be seen in the DIC concentrations for the fine grain experiments (Fig. 3). As DIC was handled with the lowest priority (regarding low sampling volumes), only a few measurements are available which makes it hard to detect trends.

Due to the experimental setup, it is only possible to give a rough estimate of the CO$_2$ drawdown effect by weathering. The

25   largest uncertainty is the available amount of water for reaction percolating the upper layers pore volume. Since the elevated elemental concentrations in the upper layer do not progress evenly downwards, it can be assumed that large quantities of water are bypassing the bulk material as preferential flow, possibly along the bucket rims and potentially through the soil facilitated by plant roots. The process of preferential flow is well established for natural soils (Beven and Germann, 2013), thus it may be considered a natural analogue in this experiment.

30   The amount of Mg released can theoretically be estimated by multiplying its concentrations with the calculated average outflow water volume at the mesocosm bottom (supplement Fig. S12). Yet, due to the preferential flow effect, only a small proportion of the precipitation water reacts continuously with the applied grains. This effect is reflected in only slightly elevated element

concentrations in the bulk outflow water, which represents the main part of the outflow (e.g. Fig. 5). The mixing with water, which predominantly has not been in contact with minerals leads to a dilution of elements in the collected solution, consequently the estimated weathering fluxes from the mesocosm and the CO_2 sequestration effect is lower as if only the upper layer's pore water concentration changes would be used to evaluate the weathering flux, assuming ideal percolation through

5   the pore space. While this may be a shortcoming of the experimental setup, there will be comparable effects in natural environments, evoked by macropores, which lead to the preferential transportation of water downwards, effectively decreasing rock-water interaction times (Nielsen et al., 1986). Comparing Mg concentrations in surface layer pore water and outlet water, the ratio is in both setups rather consistently around 13 (Tab. 3), indicating that more than 90% of the outflowing water is made up by water from preferential flow, which was not or only very shortly available for weathering reactions. The estimated total

10   annual CO_2 sequestration of maximum 4.9 t CO_2 km^{-2} a^{-1} is two orders of magnitude lower than what was observed in a soil column experiment (Renforth et al., 2015). Applied at the global scale, i.e. on all potentially available arable land (min/max taken from Moosdorf et al., 2014), this yields a comparably low CO_2 sequestration potential of maximum 0.07 Gt CO_2 a^{-1}. When the calculations are based on the corrected surface layer flux observations, values are about one order of magnitude higher (Tab. 3), which makes them comparable to lower end sequestration rates reported from a smaller pot experiment in ten

15   Berge et al. (2012). Global estimates do not take geographic variability into account. Since weathering rates are increased in (sub-) tropical regions the global potential based on temperate conditions is underestimated. Data on pCO_2 in the mesocosm soils (supplement Fig. S13) corroborates that weathering effects must be decreased compared to tropical areas as values in the experiment were 850-1300 µatm in the surface layer (depth = 5 cm) whereas they are up to thirty times higher in areas with high evapotranspiration (Brook et al., 1983).

20   The large stretch of results shows a) that the preferential flow effect is an important parameter to include in flux estimates at larger scales, which was not considered so far, and b) that it is fundamental for such an experiment setup to monitor the water fluxes through the entire pot.

4.3 Trace elements and processes

The release of trace metals which can be potentially harmful to the environment was mentioned as one of the side effects of

25   terrestrial Enhanced Weathering (Hartmann et al., 2013). The effect is especially pronounced when rocks like the dunite in this experiment are applied, since they contain larger amounts of Cr and Ni (>2000 ppm each, Tab. 1). Soil analysis confirms an increase of trace metals, which are derived from the added material. The data also shows that the lower untreated layers are little affected by the dunite treatment (Fig. 8). Focussing on Ni and Cr, which are the predominant trace metals, soil solution concentrations fluctuate strongly (Fig. 9) due to warmer periods and subsequent drying-out and enrichment of dissolved

30   elements. The dissolution of dunite leads to elevated levels of Ni and Cr concentrations in the soil solution over the control (supplement Fig. S15).

Ni is mobile at the measured pH values, reflected in concentrations which exceed drinking water quality thresholds in the surface layer, e.g. formulated by the WHO (2011) with 0.02 mg L^{-1} ($\hat{=}$ 339.2 nmol L^{-1}), yet is within the recommended limits for agricultural irrigation water (0.2 mg L-1, Ayers and Westcot, 1985). This demonstrates that a close monitoring of the affected waters is necessary to understand implications of a widespread deployment of EW with materials containing elevated

5   concentrations of mobile trace metals.

When comparing the theoretical Mg/Ni ratio in the olivine with measured data in the soil solution of the surface layer (Tab. 5), it can be shown that less Ni is mobilized than theoretically possible (factor 10 – 20 difference, depending on the grain size). Under the given physico-chemical conditions it is possible that Fe- and Al-Hydroxides lead to the partial sorption of Ni (Rieuwerts, 2007). Furthermore, the incongruent release of Ni can probably be attributed to the incongruent dissolution of the

10 dunite powder as it is composed of olivine (up to 92% forsterite) and trace minerals like chlorite, enstatite, and serpentine. Dissolution rates vary by mineral and additionally, Ni contents within the minerals crystallographic structure are highly variable. The different dissolution rates plus the compositional variability directly impact the cation release of the whole applied rock material, especially the trace metals release, and may explain the differences between idealized stochiometric Mg/Ni release ratios and measured Mg/Ni release ratios in the pore water.

15 **Tab. 5: Preferential release of Ni over Mg during the dissolution of dunite. Molar ratios of Mg/Ni. Values for fine/coarse setups are averaged over the experimental period.**

	rock	surface layer solution	
		fine setup	coarse setup
	[mol kg^{-1}]	[µmol kg^{-1}]	[µmol kg^{-1}]
Mg	11.2	4175	638
Ni	0.05	1.03	0.26
Mg/Ni molar ratio	224	4053	2454

At the same time, Cr is apparently less mobile (supplement Fig. S15) in the mesocosm experiment, considering the sample approach, which is matching the general behavior of Cr mobility at pH values measured in the soils (7-9; Kabata-Pendias (1993)). However, elevated Cr values have been reported for a column experiment, which is to some extent comparable to the

20 mesocosms. In contrast to our experiment, values increased stronger by up to 9 ng g^{-1} ($\approx$ 173 nmol kg^{-1}), including background Cr (Renforth et al., 2015). Interestingly, Cr seems to be actively removed from the solution at a later stage of the experiment, shown by Cr concentrations in the untreated mesocosms being higher than in the treated mesocosms (Fig. 9a), probably due to the higher pH compared to the control.

If the trace elements within the applied olivine remain immobile, they accumulate in the soils and can potentially be released

25 at dropping pH values or changing redox conditions (McClain and Maher, 2016 and references therein). Grain size effects are visible, showing increased concentrations of Ni in the mesocosms amended with fine olivine. Other trace elements are represented only in smaller amounts in the composition of the source rock, thus, not releasing significant amounts of material to the pore waters.

Overall these findings from the mesocosm experiment underline the proposition to focus on alternative sources like basalt (Hartmann et al., 2013; Taylor et al., 2015; Strefler et al., 2018) to avoid strong environmental impacts from trace element release.

5 Conclusion

5   Given the scarcity of data considering the field application of rock material for Enhanced Weathering, there are some lessons to be learned from this experiment. It could be shown that there is a sequestration effect and the order of magnitude is potentially large enough for the method to be considered to be one piece in the puzzle of negative emission technology portfolios. However, the calculations are bound to high uncertainties mainly from water flow estimates. It is crucial to deal with irrigation water bypass in mesocosms if reliable weathering rates should be calculated. The analyses shown here indicate

10   the relevance of including preferential flow in future flux calculations, even if it may be lower in more natural environments. One of the main concerns of the rock powder application is the release of potentially harmful trace elements. It could be shown for the first time in a dedicated experiment, that levels of Ni in solution are significantly elevated whereas it was possible to confirm that Cr mobilization is low under the given soil conditions.

The experiment also showed that the behavior of silica in the soil is not well understood if silicate powder of fine grain size is

15   applied. This is evidenced by the high Mg/Si ratios and the potential sink of silica in comparison to the non-silicate treated mesocosms. We hypothesize that physico-chemical processes, like the formation of a cation depleted and Si enriched grain surface layer, are responsible for the missing silica. The available data do not allow further conclusions.

Overall, this shows that mesoscale and field experiments are of utmost importance to identify the essential processes, to decrease uncertainties, and to address the effects of elevated element fluxes. Only if budgets of EW can be estimated reliably,

20   the resulting CO_2 consumption could be bound to a carbon prize within a NET deployment strategy.

Competing interests

The authors declare that they have no conflict of interest.

Author contribution statements

This article was conceived by the joint work of E.S., J.S., J.H., and T.A., which all participated in discussions, planning and

25   writing, with the lead of T.A.. The mesocosm study was conceived and designed by E.S., J.S., P.M., and I.J.. Sampling was primarily conducted by E.S. and J.S.. Mg and Si analyses were done by E.S. and J.S., trace elements were analyzed by E.K.F., DIC was measured by T.A.. W.O.G. contributed to the discussion of trace elements. J.H. contributed to the discussion of weathering effects.

Acknowledgments

This research was executed with the financial support of the Research Foundation Flanders (FWO), project no. G043313N 'Silicate fertilization, crop production and carbon storage: a new and integrated concept for sustainable management of agricultural ecosystems'. J.S. is a postdoctoral fellow of FWO (project no. 12H8616N). Additional funds were provided by the German Research Foundation's priority program DFG SPP 1689 on "Climate Engineering–Risks, Challenges and Opportunities?" and specifically the CEMICS2 project. Further support came from the DFG Cluster of Excellence 'CliSAP', EXC177, Universität Hamburg.

We acknowledge Peggy Bartsch, Tom Jäppinen, Marvin Keitzel, and Andreas Weiss for valuable contributions from the wet lab, and Sebastian Lindhorst for providing granulometric analyses (all from Institute for Geology, Universität Hamburg). We thank Stephan Jung and Joachim Ludwig (from Institute for Mineralogy and Petrography, Universität Hamburg) for contributing the XRF and XRD analyses.

References

Anda, M., Shamshuddin, J., and Fauziah, C. I.: Increasing negative charge and nutrient contents of a highly weathered soil using basalt and rice husk to promote cocoa growth under field conditions, Soil and Tillage Research, 132, 1-11, http://dx.doi.org/10.1016/j.still.2013.04.005, 2013.

Anda, M., Shamshuddin, J., and Fauziah, C. I.: Improving chemical properties of a highly weathered soil using finely ground basalt rocks, CATENA, 124, 147-161, http://dx.doi.org/10.1016/j.catena.2014.09.012, 2015a.

Anda, M., Suryani, E., Husnain, and Subardja, D.: Strategy to reduce fertilizer application in volcanic paddy soils: Nutrient reserves approach from parent materials, Soil and Tillage Research, 150, 10-20, http://dx.doi.org/10.1016/j.still.2015.01.005, 2015b.

Ayers, R. S., and Westcot, D. W.: Water quality for agriculture, Food and Agriculture Organization of the United Nations, Rome, 1985.

Beerling, D. J.: Enhanced rock weathering: biological climate change mitigation with co-benefits for food security?, Biology Letters, 13, 20170149, 10.1098/rsbl.2017.0149, 2017.

Beerling, D. J., Leake, J. R., Long, S. P., Scholes, J. D., Ton, J., Nelson, P. N., Bird, M., Kantzas, E., Taylor, L. L., Sarkar, B., Kelland, M., DeLucia, E., Kantola, I., Muller, C., Rau, G., and Hansen, J.: Farming with crops and rocks to address global climate, food and soil security, Nat Plants, 10.1038/s41477-018-0108-y, 2018.

Berner, R. A.: The long-term carbon cycle, fossil fuels and atmospheric composition, Nature, 426, 323-326, 10.1038/nature02131, 2003.

Beven, K., and Germann, P.: Macropores and water flow in soils revisited, Water Resources Research, 49, 3071-3092, 10.1002/wrcr.20156, 2013.

Brook, G. A., Folkoff, M. E., and Box, E. O.: A World Model Of Soil Carbon Dioxide, Earth Surface Processes And Landforms, 8, 79-88, 1983.

Brunauer, S., Emmett, P. H., and Teller, E.: Adsorption of Gases in Multimolecular Layers, Journal of the American Chemical Society, 60, 309-319, 10.1021/ja01269a023, 1938.

Casey, W. H., Westrich, H. R., Banfield, J. F., Ferruzzi, G., and Arnold, G. W.: Leaching and Reconstruction at the Surfaces of Dissolving Chain-Silicate Minerals, Nature, 366, 253-256, DOI 10.1038/366253a0, 1993.

Ciceri, D., and Allanore, A.: Local fertilizers to achieve food self-sufficiency in Africa, Sci. Total Environ., 648, 669-680, https://doi.org/10.1016/j.scitotenv.2018.08.154, 2019.

Cordell, D., Drangert, J.-O., and White, S.: The story of phosphorus: Global food security and food for thought, Global Environmental Change, 19, 292-305, 10.1016/j.gloenvcha.2008.10.009, 2009.

Cregan, P., Hirth, J., and Conyers, M.: Amelioration of Siol Acidity by Liming and other Amendments, in: Soil Acidity and Plant Growth, edited by: Robson, A., Academic Press Australia, Marrickville, 1989.

Daval, D., Sissmann, O., Menguy, N., Saldi, G. D., Guyot, F., Martinez, I., Corvisier, J., Garcia, B., Machouk, I., Knauss, K. G., and Hellmann, R.: Influence of amorphous silica layer formation on the dissolution rate of olivine at 90 °C and elevated pCO2, Chemical Geology, 284, 193-209, http://dx.doi.org/10.1016/j.chemgeo.2011.02.021, 2011.

Daval, D., Hellmann, R., Martinez, I., Gangloff, S., and Guyot, F.: Lizardite serpentine dissolution kinetics as a function of pH and temperature, including effects of elevated pCO2, Chemical Geology, 351, 245-256, http://dx.doi.org/10.1016/j.chemgeo.2013.05.020, 2013a.

Daval, D., Hellmann, R., Saldi, G. D., Wirth, R., and Knauss, K. G.: Linking nm-scale measurements of the anisotropy of silicate surface reactivity to macroscopic dissolution rate laws: New insights based on diopside, Geochim Cosmochim Ac, 107, 121-134, http://dx.doi.org/10.1016/j.gca.2012.12.045, 2013b.

de Oliveira Garcia, W., Amann, T., and Hartmann, J.: Increasing biomass demand enlarges negative forest nutrient budget areas in wood export regions, Scientific reports, 8, 5280, 10.1038/s41598-018-22728-5, 2018.

De Villiers, O. D. H.: Soil rejuvenation with crushed basalt in Mauritius, Int sugar J, 63, 363-364, 1961.

Edwards, D. P., Lim, F., James, R. H., Pearce, C. R., Scholes, J., Freckleton, R. P., and Beerling, D. J.: Climate change mitigation: potential benefits and pitfalls of enhanced rock weathering in tropical agriculture, Biology Letters, 13, 20160715, 10.1098/rsbl.2016.0715, 2017.

Fuss, S., Canadell, J. G., Peters, G. P., Tavoni, M., Andrew, R. M., Ciais, P., Jackson, R. B., Jones, C. D., Kraxner, F., Nakicenovic, N., Le Quere, C., Raupach, M. R., Sharifi, A., Smith, P., and Yamagata, Y.: Betting on negative emissions, Nature Clim. Change, 4, 850-853, 10.1038/nclimate2392, 2014.

Fuss, S., Lamb, W. F., Callaghan, M. W., Hilaire, J., Creutzig, F., Amann, T., Beringer, T., de Oliveira Garcia, W., Hartmann, J., Khanna, T., Luderer, G., Nemet, G. F., Rogelj, J., Smith, P., Vicente, J. L. V., Wilcox, J., del Mar Zamora Dominguez, M., and Minx, J. C.: Negative emissions—Part 2: Costs, potentials and side effects, Environmental Research Letters, 13, 10.1088/1748-9326/aabf9f, 2018.

Hartmann, J., Jansen, N., Kempe, S., and H. Dürr, H.: Geochemistry of the river Rhine and the upper Danube: Recent trends and lithological influence on baselines, Journal of Environmental Science for Sustainable Society, 1, 39-46, 2007.

Hartmann, J., Levy, J., and Kempe, S.: Increasing dissolved silica trends in the Rhine River: an effect of recovery from high P loads?, Limnology, 12, 63-73, 10.1007/s10201-010-0322-4, 2011.

Hartmann, J., West, A. J., Renforth, P., Köhler, P., De La Rocha, C. L., Wolf-Gladrow, D. A., Dürr, H. H., and Scheffran, J.: Enhanced chemical weathering as a geoengineering strategy to reduce atmospheric carbon dioxide, supply nutrients, and mitigate ocean acidification, Rev Geophys, 51, 113-149, 10.1002/Rog.20004, 2013.

Haynes, R. J., and Naidu, R.: Influence of lime, fertilizer and manure applications on soil organic matter content and soil physical conditions: a review, Nutr Cycl Agroecosys, 51, 123-137, Doi 10.1023/A:1009738307837, 1998.

Heinrichs, H., and Herrmann, A. G.: Praktikum der analytischen Geochemie, Springer-Verlag, 2013.

Hellmann, R., Wirth, R., Daval, D., Barnes, J.-P., Penisson, J.-M., Tisserand, D., Epicier, T., Florin, B., and Hervig, R. L.: Unifying natural and laboratory chemical weathering with interfacial dissolution–reprecipitation: A study based on the nanometer-scale chemistry of fluid–silicate interfaces, Chemical Geology, 294–295, 203-216, http://dx.doi.org/10.1016/j.chemgeo.2011.12.002, 2012.

Kabata-Pendias, A.: Behavioral Properties of Trace-Metals in Soils, Applied Geochemistry, Supplementary Issue No 2, January 1993, 3-9, 1993.

Kantola, I. B., Masters, M. D., Beerling, D. J., Long, S. P., and DeLucia, E. H.: Potential of global croplands and bioenergy crops for climate change mitigation through deployment for enhanced weathering, Biology Letters, 13, 20160714, 10.1098/rsbl.2016.0714, 2017.

Köhler, P., Hartmann, J., and Wolf-Gladrow, D. A.: Geoengineering potential of artificially enhanced silicate weathering of olivine, P Natl Acad Sci USA, 107, 20228-20233, 10.1073/pnas.1000545107, 2010.

Kronberg, B. I.: The geochemistry of some Brazilian soils and geochemical considerations for agriculture on highly leached soils, 1977.

Leonardos, O. H., Fyfe, W. S., and Kronberg, B. I.: The use of ground rocks in laterite systems: An improvement to the use of conventional soluble fertilizers?, Chemical Geology, 60, 361-370, http://dx.doi.org/10.1016/0009-2541(87)90143-4, 1987.

Lightfoot, D. R.: The Nature, History, and Distribution of Lithic Mulch Agriculture: An Ancient Technique of Dryland Agriculture, The Agricultural History Review, 44, 206-222, 10.2307/40275100, 1996.

Maher, K., Johnson, N. C., Jackson, A., Lammers, L. N., Torchinsky, A. B., Weaver, K. L., Bird, D. K., and Brown, G. E.: A spatially resolved surface kinetic model for forsterite dissolution, Geochim Cosmochim Ac, 174, 313-334, 10.1016/j.gca.2015.11.019, 2016.

Manning, D. A. C.: How will minerals feed the world in 2050?, Proceedings of the Geologists' Association, 126, 14-17, http://dx.doi.org/10.1016/j.pgeola.2014.12.005, 2015.

McClain, C. N., and Maher, K.: Chromium fluxes and speciation in ultramafic catchments and global rivers, Chemical Geology, 426, 135-157, 10.1016/j.chemgeo.2016.01.021, 2016.

Meybeck, M.: Global analysis of river systems: from Earth system controls to Anthropocene syndromes., Philosophical transactions of the Royal Society of London. Series B, Biological sciences, 358, 1935-1955, 10.1098/rstb.2003.1379, 2003.

Minx, J. C., Lamb, W. F., Callaghan, M. W., Fuss, S., Hilaire, J., Creutzig, F., Amann, T., Beringer, T., de Oliveira Garcia, W., Hartmann, J., Khanna, T., Lenzi, D., Luderer, G., Nemet, G. F., Rogelj, J., Smith, P., Vicente Vicente, J. L., Wilcox, J., and del Mar Zamora Dominguez, M.: Negative emissions—Part 1: Research landscape and synthesis, Environmental Research Letters, 13, 10.1088/1748-9326/aabf9b, 2018.

Montserrat, F., Renforth, P., Hartmann, J., Leermakers, M., Knops, P., and Meysman, F. J. R.: Olivine dissolution in seawater: implications for CO2 sequestration through Enhanced Weathering in coastal environments, Environmental Science & Technology, 51, 3960-3972, 10.1021/acs.est.6b05942, 2017.

Moosdorf, N., Renforth, P., and Hartmann, J.: Carbon dioxide efficiency of terrestrial enhanced weathering, Environ Sci Technol, 48, 4809-4816, 10.1021/es4052022, 2014.

Nielsen, D. R., Th. Van Genuchten, M., and Biggar, J. W.: Water flow and solute transport processes in the unsaturated zone, Water Resources Research, 22, 89S-108S, 10.1029/WR022i09Sp0089S, 1986.

5 Nugent, M. A., Brantley, S. L., Pantano, C. G., and Maurice, P. A.: The influence of natural mineral coatings on feldspar weathering, Nature, 395, 588-591, Doi 10.1038/26951, 1998.

Peters, G. P.: The 'best available science' to inform 1.5 °C policy choices, Nature Climate Change, 6, 646-649, 10.1038/nclimate3000, 2016.

Pokrovsky, O. S., and Schott, J.: Kinetics and mechanism of forsterite dissolution at 25°C and pH from 1 to 12, Geochim Cosmochim Ac, 64, 3313-3325, 10.1016/s0016-7037(00)00434-8, 2000.

10 Prudêncio, M. I., Sequeira Braga, M. A., Paquet, H., Waerenborgh, J. C., Pereira, L. C. J., and Gouveia, M. A.: Clay mineral assemblages in weathered basalt profiles from central and southern Portugal: climatic significance, CATENA, 49, 77-89, https://doi.org/10.1016/S0341-8162(02)00018-8, 2002.

Radach, G., and Pätsch, J.: Variability of continental riverine freshwater and nutrient inputs into the North Sea for the years 1977-2000 and its consequences for the assessment of eutrophication, Estuaries and Coasts, 30, 66-81, 2007.

15 Raymond, P. A., and Cole, J. J.: Increase in the export of alkalinity from North America's largest river, Science, 301, 88-91, 2003.

Raymond, P. A., and Hamilton, S. K.: Anthropogenic influences on riverine fluxes of dissolved inorganic carbon to the oceans, Limnology and Oceanography Letters, 3, 143-155, 10.1002/lol2.10069, 2018.

Renforth, P., Pogge von Strandmann, P. A. E., and Henderson, G. M.: The dissolution of olivine added to soil: Implications for enhanced weathering, Applied Geochemistry, 61, 109-118, http://dx.doi.org/10.1016/j.apgeochem.2015.05.016, 2015.

20 Rieuwerts, J. S.: The mobility and bioavailability of trace metals in tropical soils: a review, Chemical Speciation & Bioavailability, 19, 75-85, 10.3184/095422907X211918, 2007.

Rogelj, J., Popp, A., Calvin, K. V., Luderer, G., Emmerling, J., Gernaat, D., Fujimori, S., Strefler, J., Hasegawa, T., Marangoni, G., Krey, V., Kriegler, E., Riahi, K., van Vuuren, D. P., Doelman, J., Drouet, L., Edmonds, J., Fricko, O., Harmsen, M., Havlík, P., Humpenöder, F., Stehfest, E., and Tavoni, M.: Scenarios towards limiting global mean temperature increase below 1.5 °C, Nature Climate Change, 8, 325-332, 10.1038/s41558-018-0091-3, 2018.

25 Rosso, J. J., and Rimstidt, J. D.: A high resolution study of forsterite dissolution rates, Geochim Cosmochim Ac, 64, 797-811, http://dx.doi.org/10.1016/S0016-7037(99)00354-3, 2000.

Ruiz-Agudo, E., Putnis, C. V., Rodriguez-Navarro, C., and Putnis, A.: Mechanism of leached layer formation during chemical weathering of silicate minerals, Geology, 40, 947-950, 10.1130/g33339.1, 2012.

30 Sanderson, B. M., O'Neill, B. C., and Tebaldi, C.: What would it take to achieve the Paris temperature targets?, Geophysical Research Letters, 43, 7133-7142, 10.1002/2016gl069563, 2016.

Schuiling, R. D., and Krijgsman, P.: Enhanced weathering: An effective and cheap tool to sequester CO2, Climatic Change, 74, 349-354, DOI 10.1007/s10584-005-3485-y, 2006.

Shamshuddin, J., Anda, M., Fauziah, C. I., and Omar, S. R. S.: Growth of Cocoa Planted on Highly Weathered Soil as Affected by Application of Basalt and/or Compost, Communications in Soil Science and Plant Analysis, 42, 2751-2766, 10.1080/00103624.2011.622822, 2011.

Shamshuddin, J., and Anda, M.: Enhancing the Productivity of Ultisols and Oxisols in Malaysia using Basalt and/or Compost, Pedologist, 2012, 382-391, 2012.

Smith, L. K.: Weathering of basalt: formation of iddingsite, Clays and Clay Minerals, 35, 418-428, 1987.

40 Strefler, J., Amann, T., Bauer, N., Kriegler, E., and Hartmann, J.: Potential and costs of carbon dioxide removal by enhanced weathering of rocks, Environmental Research Letters, 13, 10.1088/1748-9326/aaa9c4, 2018.

Stumm, W., and Morgan, J. J.: Aquatic Chemistry: Chemical Equilibria and Rates in Natural Waters, 3rd ed., Environmental Science and Technology, edited by: Schnoor, J. L., and Zehnder, A., John Wiley & Sons, Inc., New York, 1996.

Taylor, L. L., Quirk, J., Thorley, R. M. S., Kharecha, P. A., Hansen, J., Ridgwell, A., Lomas, M. R., Banwart, S. A., and Beerling, D. J.: 45 Enhanced weathering strategies for stabilizing climate and averting ocean acidification, Nature Climate Change, 10.1038/nclimate2882, 2015.

Taylor, L. L., Beerling, D. J., Quegan, S., and Banwart, S. A.: Simulating carbon capture by enhanced weathering with croplands: an overview of key processes highlighting areas of future model development, Biology Letters, 13, 20160868, 10.1098/rsbl.2016.0868, 2017.

ten Berge, H. F. M., van der Meer, H. G., Steenhuizen, J. W., Goedhart, P. W., Knops, P., and Verhagen, J.: Olivine Weathering in Soil, and 50 Its Effects on Growth and Nutrient Uptake in Ryegrass *Lolium perenne* L.: A Pot Experiment, PLoS ONE, 7, e42098, 10.1371/journal.pone.0042098, 2012.

van Straaten, P.: Rocks for Crops: Agrominerals of sub-Saharan Africa, ICRAF, Nairobi, Kenya, 338 pp., 2002.

Van Straaten, P.: Farming with rocks and minerals: challenges and opportunities, Anais da Academia Brasileira de Ciencias, 78, 731-747, 2006.

55 Guidelines for drinking-water quality (4th edition), 2011.

Wogelius, R. A., and Walther, J. V.: Olivine Dissolution Kinetics at near-Surface Conditions, Chemical Geology, 97, 101-112, Doi 10.1016/0009-2541(92)90138-U, 1992.